Stabilizing Frame Slotted Aloha-Based IoT Systems: A Geometric Ergodicity Perspective

Jihong Yu, *Member, IEEE*, Pengfei Zhang, Lin Chen, *Member, IEEE*, Jiangchuan Liu, *Fellow, IEEE*, Rongrong Zhang, Kehao Wang, and Jianping An, *Member, IEEE*

***Abstract*— The explosive deployment of the Internet of Things (IoT) brings a massive number of light-weight and energy-limited IoT devices, challenging stable wireless access. Energy-efficient, Frame Slotted Aloha (FSA) recently emerged as a promising MAC protocol for large-scale IoT systems such as Machine to Machine (M2M) and Radio Frequency Identification (RFID). Yet the stability of FSA and how to stabilize it, despite of its fundamental importance on the effective operation in practical systems, have not been systematically addressed. In order to bridge this gap, we devote this paper to designing stable FSA-based access protocol (SFP) to stabilize IoT systems. We first design an additive active node population estimation scheme and use the estimate to set frame size and participation probability for throughput optimization. We then carry out theoretical analysis demonstrating the stability of SFP in the sense of geometric ergodicity of Markov chain derived from dynamics of the active node population and its estimate. Our central theoretical result is a set of closed-form conditions on the stability of SFP. We further conduct extensive simulations whose results confirm our theoretical analysis and demonstrate the effectiveness of SFP.**

***Index Terms*— IoT, massive access, frame slotted aloha.**

I. Introduction

IoT systems like M2M [10] and RFID [2], [19] have attracted considerable research attention due to their ability of ubiquitous sensing and low energy consumption. Compared to the traditional human-centric communication paradigm, an IoT system needs to accommodate a massive number of inter-connected nodes in many cases. In such densely deployed scenarios, how to enable the system operating around a stable equilibrium is a pivotal challenge for any IoT wireless access protocol. Motivated by this challenge, we embark in this paper on a comprehensive study on the *stability* of wireless access in IoT systems. To make our analysis practically applicable, we instantiate our framework by focusing on Frame Slotted Aloha (FSA), which is regarded as the *de facto* MAC protocol to coordinate massive access in M2M communications [5], [13] and RFID systems [17], [18]. Especially, FSA plays a fundamental role in node identification and is standardized in the EPCGlobal Class-1 Generation-2 (C1G2) RFID standard [3].

Architecturally, an FSA-based communication system consists of two types of devices: a *Coordinator* that configures system parameters and controls communications, and a large number of *nodes* that communicate with the Coordinator. FSA organizes multiple consecutive time slots into a *frame*. At the beginning of a frame, the coordinator broadcasts the system parameters such as frame size and participation probability. If a node has a packet, referred to as *active node*, it will decide whether to send the packet with the received participation probability. Note that each active node is allowed to transmit only a single packet per frame in a randomly chosen time slot.

Due to its wide applications, a large body of studies have been devoted to performance analysis of FSA in both static and dynamic systems. However, very limited work has been done on the stabilization of FSA in dynamic systems with the presence of new traffic despite its fundamental importance both on the theoretical characterisation of FSA performance and its effective operation in practice. The existing works [1], [5], [11] considering static systems without new arrivals mainly derive the optimal frame size and throughput. In dynamic systems, the works [15], [16] analyze the throughput and stability conditions of FSA, respectively, but they do not study how to stabilize FSA with presence of unknown number of active nodes and how node population estimation influences the stability (c.f. Table I summarizing limitations of the existing works and c.f. Sec.VI on detailed related works). Therefore, we argue that a systematic study on the FSA stabilization is called for so as to lay theoretical foundations for design and optimization of FSA based IoT systems.

Technically, there are two main challenges in designing unified stable FSA protocol:

1) *System dynamics with unknown new traffic arrivals:* The Coordinator must know the number of active nodes in the system to configure FSA parameters for throughput maximization and stability. Practical systems, however,

Manuscript received January 17, 2020; revised June 2, 2020; accepted July 17, 2020. Date of publication August 24, 2020; date of current version February 17, 2021. This work was supported in part by the NSF of China under Grant 61901035 and Grant 61801064, and in part by the Beijing Institute of Technology Research Fund Program for Young Scholars and Young Elite Scientist Sponsorship Program by CAST and Chongqing Key Laboratory of Mobile Communications Technology. The work of Rongrong Zhang and Kehao Wang was supported in part by the Science and Technology Project of Beijing Municipal Education Commission under Grant KM202010028005, and in part by the NSF of China under Grant 61672395. *(Corresponding authors: Jihong Yu; Kehao Wang.)*

Jihong Yu, Pengfei Zhang, and Jianping An are with the School of Information and Electronics, Beijing Institute of Technology, Beijing 100081, China (e-mail: jihong.yu@bit.edu.cn; zhangpf14@bit.edu.cn; an@bit.edu.cn).

Lin Chen is with the School of Data and Computer Science, Sun Yat-sen University, Guangzhou 510275, China (e-mail: chenlin69@mail.sysu.edu.cn).

Jiangchuan Liu is with the School of Computing Science, Simon Fraser University, Burnaby, BC V5A 1S6, Canada (e-mail: jcliu@sfu.ca).

Rongrong Zhang is with Information Engineering College, Capital Normal University, Beijing 100048, China (e-mail: zhangrr@cnu.edu.cn).

Kehao Wang is with the Department of Information Engineering, Wuhan University of Technology, Wuhan 430070, China (e-mail: kehao.wang@whut.edu.cn).

Color versions of one or more of the figures in this article are available online at https://ieeexplore.ieee.org.

Digital Object Identifier 10.1109/JSAC.2020.3018795

TABLE I
SUMMARY OF EXISTING WORKS ON FSA

Existing works	New arrivals	Unknown population	Stability guarantee
[20], [21], [1], [5]	×	×	×
[15], [13]	✓	×	×
[11]	×	✓	×
[16]	✓	✓	×
Our work: SFP	✓	✓	✓

experience system dynamics, such as new traffic arrivals due to triggered events. In such dynamic systems, the Coordinator cannot know node population *a priori*. Most of existing protocols either assume the known node population [1] or study the scenarios without new arrivals [5]. Therefore, designing a unified FSA stabilization framework for dynamic systems with unknown node population is a first technical cornerstone in designing effective FSA-based access protocols.

2) *Frame-based measurement and control:* FSA operates in a frame-after-frame pattern, making its stabilization more challenging. Specifically, the Coordinator can learn the states of the slots in the frame. In order to accurately track the node population the statistic characteristics of multiple slots needs to be derived. This is different from traditional methods based on slot-level feedback (e.g., empty, successful, collision) [4], [9] for Slotted Aloha, making them inapplicable for FSA. It is then crucial to choose the appropriate frame-level feedback to learn system dynamics.

Motivated by the above challenges, we design a stable FSA-based access protocol (SFP) which works on top of FSA by integrating nodes' transmissions and node population estimation to stabilize FSA and achieve maximum throughput. With SFP, the Coordinator can obtain a bitmap from the nodes' transmissions at the end of a frame and then can leverage the number of empty slots and an additive estimation scheme to evaluate the change of the active node population and to update parameters in order to stabilize the protocol. The main contributions of this paper are articulated as follows:

- We propose the first FSA-based access control protocol for dynamic systems with **proven** stability. The protocol can estimate the number of nodes and use the estimate to configure frame size and participation probability such that throughput is maximized and stability is guaranteed.
- We analytically demonstrate that our proposed protocol SFP can be stabilized in the sense of ergodicity of Markov chain under two conditions: (1) the parameters of SFP are tuned by the parameter configuration rule (c.f. Sec. IV-C); (2) the normalized arrival rate is smaller than $1/e$.
- We develop an additive estimator for node population estimation in FSA based dynamic systems with proven performance in terms of accuracy and convergence.

II. SYSTEM MODEL AND PROBLEM FORMULATION

In this section, we introduce generic model of FSA-based IoT systems and formulate its stability from the perspective of geometric ergodicity.

A. FSA Based Random Access

We consider a system of identical nodes with buffer capacity of one packet and operating on one frequency channel. A node has backlog will not generate new data while a random number of the remaining nodes generate a packet following the traffic model introduced shortly. FSA organizes a number of consecutive time slots to form a frame. At each frame, each node independently selects a slot at random to send its packet at most once per frame. Backlogs and new arrivals in the current frame will be sent in the following frame. Note that if a node sends its packet successfully, it will keep silent until new data arrives. More specifically, in an FSA-based communication system, the Coordinator, such as base station/gateway in M2M systems and reader in RFID systems, queries nodes in frame t with frame size f_t and participation probability p_t. We denote the number of slots in frame t by f_t. With these parameters, each active node has a probability of p_t to take part in this frame. If determining to participate, it selects a slot in the frame uniformly at random to transmit its packet. We assume that the length of a slot is long enough for one packet transmission.

As each node responds independently, a slot may experience three states depending on the number of nodes responding in this slot. If none of nodes replies, this slot is referred to as *empty* slot; if only one node replies in this slot, it is called a *successful* slot; if multiple nodes reply in this slot, it is called a *collision* slot. When a frame ends, the Coordinator can get states of all slots in this frame.

In FSA-based systems, the Coordinator controls the random access by adaptively adjusting the frame size f_t and/or the participation probability p_t. At the end of frame t, the Coordinator determines the frame size and the participation probability for frame $t+1$ based on the access outcomes in current frame. The objective is to maximize throughput that is the average number of success packets in a unit time, which can be accomplished if it is true for the number of active nodes W_t and the frame size f_t and the participation probability p_t that $f_t/p_t = W_t$. The Coordinator, however, has no knowledge of W_t and has to predict it from the access outcomes in the previous frame and use its estimate $\hat{W}_t$ to configure the parameters.

Traffic Model: We consider a dynamic system where the number of nodes that need to send message changes. These nodes are referred to as active node. And the change may be resulted from activation/sleep depending on whether certain events are triggered. Let random variable A_t denote the total number of new arrivals during frame t and denote by A_{tl} the number of new arrivals in time slot l in frame t where $l = 1, 2, \cdots, f_t$. Assume that $(A_{tl})_{1\le l\le f_t}$ are independent and identically distributed random variables, which is exponential-type[1] with probability distribution $P\{A_{tl} = u_l\} = \lambda_{u_l}(u \ge 0)$ such that the expected number of new arrivals per time slot $\lambda = \sum_1^\infty u_l\lambda_{u_l}$ is finite. Then as $A_t = \sum_{l=1}^{f_t} A_{tl}$, the expected number of arrivals during a frame is $f_t\lambda$.

[1]The definition of exponential type for a random variable is stated in Lemma 4. The exponential-type random variables are common, such as Poisson distribution, Normal distribution, and Hyperexponential distribution.

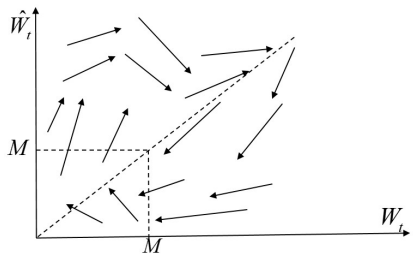

Fig. 1. Drift in the Markov Process. The value of W_t and $\hat{W}_t$ would converge to a compact set while their ratio fluctuates around 1.

B. Problem Definition

In this paper, our objective is to design a stable FSA-based protocol while proving its stability. This protocol would provide an estimator for the Coordinator to estimate the active node population and use it to set frame size and participation probability such that the throughput is maximized.

Since W_{t+1} and its estimate $\hat{W}_{t+1}$ only depend on the information from frame t, namely W_t, $\hat{W}_t$ and all slot states of this frame, the discrete-time system dynamics $(W_t)_{t\geq 0}$ and estimation process $(\hat{W}_t)_{t\geq 0}$ perform as a Markov chain on a countable state space $Z_t = (W_t, \hat{W}_t)$. The problem we solve is to guarantee the stability of the proposed FSA-based protocol. Following definition of stability in Slotted Aloha [12], we define the stability of FSA-based protocols as follows.

Definition 1: An FSA-based protocol is stable if Markov chain $(Z_t)_{t\geq 0}$ is geometrically ergodic.

Remark: By Definition 1, we can transform the study of stability of a control scheme into investigating the geometrical ergodicity of Markov chain. The rationality of this transformation is two-fold. One interpretation is the property of geometrical ergodicity that there exists an unique stationary distribution of a Markov chain if it is ergodic. The other can be interpreted from the nature of geometrical ergodicity that recurrent time of the chain to a finite set is exponential-type.

We use Fig. 1 to illustrate geometrical ergodicity of Z_t. The arrows denote the mean one-step change of $(W_t, \hat{W}_t)$, referred as drift. We can interpret geometrical ergodicity as follows: First, $\hat{W}_t$ would track the change of W_t so that their ratio keeps around 1. Second, once the value of W_t increases, the drift would decrease pushing W_{t+1} towards the finite set, e.g., the square in the figure, and the speed is exponential.

Overview of Proposed Solution: The main technical part is two-fold: FSA-based protocol and its stability analysis. 1) The protocol contains FSA mechanism and a node population estimator. We first study the statistical characteristics of the number of empty and successful slots in a frame, enabling that the Coordinator can learn a combination of frame size and participation probability that maximizes throughput. With such settings, the Coordinator can predict the expected number of empty slots. If the difference between this predicted value and the measured one exceeds a threshold, the Coordinator learns an inaccurate estimate and will correct it. 2) The stability is proven in three steps: we model the Markov chain of system states $(W_t, \hat{W}_t)$; we investigate the properties of one-frame drift; we analyze multi-frame Lyapunov drift to prove the ergodicity of the Markov chain. The derived stability conditions provide guideline on protocol parameter configuration.

III. SFP: Stable FSA-Based Protocol

In this section, we present a stable FSA-based protocol, referred to as *SFP, which contains FSA mechanism and a node population estimator with proven parameter configuration*. We first formulate the statistical characteristics of FSA and use them to design the node population estimator. We then prove the stability of SFP and investigate parameter configuration to guarantee the stability.

A. Statistical Characteristics of FSA

In contrast to traditional Slotted Aloha, FSA organizes the access in frames and its access outcomes that are useful for estimation in FSA are not states of one slot, but the statistics of states of all slots, such as the number of empty slots and success slots, in the whole frame.

Let n_t and $\hat{n}_t$ denote the value of W_t and $\hat{W}_t$, respectively, i.e., the number of nodes transmitting packets in frame t and its estimate. Given the frame size f_t and the participation probability p_t, we calculate in Lemma 1 the probability that a slot in frame t is b_t where $b_t = 0$ or 1 stands for an empty slot or a successful slot, respectively.

Lemma 1: Let n_t nodes each uniformly select a slot among f_t slots at random and transmit in the chosen slot with probability p_t. Let $q_t(b_t)$ be the probability that a slot in frame t is b_t. For a large n_t, it holds that

$$q_t(b_t) = \begin{cases} (1-\frac{p_t}{f_t})^{n_t} \approx e^{-\frac{n_t p_t}{f_t}}, & \text{if } b_t = 0 \\ \frac{n_t p_t}{f_t}(1-\frac{p_t}{f_t})^{n_t-1} \approx \frac{n_t p_t}{f_t} e^{-\frac{n_t p_t}{f_t}}, & \text{if } b_t = 1. \end{cases} \tag{1}$$

Proof: The event that a node does not reply in a given slot of a frame happens when this node does not participate in this frame or it participates but does not choose this slot to reply. The probability of the former part is $1-p_t$ while that of the latter is $p_t(1-\frac{1}{f_t})$. As a result, this event happens with the probability of $1-\frac{p_t}{f_t}$. Since the event of an empty slot happens when all nodes do not choose it, we have $q_t(0) \approx e^{n_t p_t/f_t}$ for a large n_t. On the other hand, a given slot is a successful slot if there is only one node replying in this slot, which occurs with the probability of $n_t p_t f_t e^{-\frac{n_t p_t}{f_t}}$ for a large n_t. □

Having calculated the probability of an empty slot, we proceed to study its statistical properties.

Lemma 2: Denote the number of empty slots in frame t by Y_t, it holds that if n_t and $\frac{f_t}{p_t}$ are large enough and $\frac{n_t p_t}{f_t} < \infty$,

$$Y_t \sim \mathcal{N}[\mu_t, \sigma_t^2] \tag{2}$$

$$\mu_t = f_t e^{-\frac{n_t p_t}{f_t}}, \quad \sigma_t^2 = f_t e^{-\frac{n_t p_t}{f_t}}(1 - e^{-\frac{n_t p_t}{f_t}}). \tag{3}$$

Proof: The proof consists of two parts: calculating the expectation and variance of Y_t and proving the normal distribution. We first compute μ_t and σ_t^2. To this end, we use $X_t(i)$ to indicate whether a slot i in the frame t is an empty slot.

$$X_t(i) = \begin{cases} 1, & \text{if slot } i \text{ is } b_t = 0 \\ 0, & \text{otherwise.} \end{cases}$$

The number of empty slots in the whole frame, defined as Y_t, can be calculated as $Y_t = \sum_{i=1}^{f_t} X_t(i)$. As each slot i in the frame t has probability $q_t(0)$ of being an empty slot, we can compute the expectation of Y_t as

$$\mu_t = E\Big[\sum_{i=1}^{f_t} X_t(i)\Big] = \sum_{i=1}^{f_t} E\left[X_t(i)\right] = f_t e^{-\frac{n_t p_t}{f_t}}. \quad (4)$$

We next compute the variance of Y_t from general expression for variance of sum of multiple random variables that

$$\sigma_t^2 = \sum_{i=1}^{f_t} \mathrm{Var}\left[X_t(i)\right] + 2\sum_{j=2}^{f_t}\sum_{\forall i<j} \mathrm{Cov}[X_t(i), X_t(j)].$$

Since $\mathrm{Var}\left[X_t(i)\right] = E\left[X_t^2(i)\right] - E[X_t(i)]^2$, we have

$$\mathrm{Var}\left[X_t(i)\right] = e^{-\frac{n_t p_t}{f_t}} - e^{-\frac{2n_t p_t}{f_t}} = e^{-\frac{n_t p_t}{f_t}}(1 - e^{-\frac{n_t p_t}{f_t}}). \quad (5)$$

Recall (4), as it holds for $i \neq j$ that $E[X_t(i)X_t(j)] = e^{-\frac{2n_t p_t}{f_t}}$, we have $\mathrm{Cov}[X_t(i), X_t(j)] = 0$. As a result,

$$\sigma_t^2 = f_t e^{-\frac{n_t p_t}{f_t}}(1 - e^{-\frac{n_t p_t}{f_t}}), \quad (6)$$

implying the independence among slots in large-scale systems.

As a slot is empty with probability of $p_t(0)$ independent from the others, Y_t follows Binomial distribution $B(f_t, p_t(0))$ which can be approximated to a Normal distribution [8]. This completes the proof of the lemma. □

Similarly, denote by S_t the number of successful slots in frame t, we observe that S_t also follows Binomial distribution $B(f_t, q_t(1))$ with the expectation and variance as follows

$$E[S_t] = n_t p_t e^{-\frac{n_t p_t}{f_t}} \quad (7)$$

$$Var[S_t] = n_t p_t e^{-\frac{n_t p_t}{f_t}}(1 - \frac{n_t p_t}{f_t} e^{-\frac{n_t p_t}{f_t}}) \quad (8)$$

B. Framework of Node Population Estimator

As a successful slot, i.e., $b_t = 1$, means that a node sends its message to the Coordinator successfully in the frame t, $q_t(1)$ implies the throughput in this frame. Consequently, we tune f_t and p_t so that $q_t(1)$ can be maximized, which happens when $\frac{f_t}{p_t} = n_t$. Yet the Coordinator does not know n_t a prior, so we use the estimated value $\hat{n}_t$ and set $\frac{f_t}{p_t} = \hat{n}_t$. We set f_t to a constant and vary p_t such that this equation is established, which will be analyzed shortly. Hereafter, we define $\frac{n_t p_t}{f_t} = \frac{n_t}{\hat{n}_t} = \rho_t$, which means the average number of nodes replying in a slot of frame t.

At the beginning of frame t, the Coordinator broadcasts frame size f_t and participation probability p_t, and can measure the actual number of empty slots at the end of the frame. With the setting $\frac{f_t}{p_t} = \hat{n}_t$, the number of observed empty slots is expected to concentrate around its expectation $\mu_t|_{\rho_t=1}$ if the estimated value $\hat{n}_t$ is accurate. In contrast, if $\hat{n}_t$ is larger than n_t, there will be more empty slots than $\mu_t|_{\rho_t=1}$. This can be interpreted as follows: Under the constraint of $\frac{f_t}{p_t} = \hat{n}_t$ for a constant f_t, a greater $\hat{n}_t$ makes p_t lower, decreasing the probability p_t/f_t of nodes replying in a slot and thus leading to more empty slots on average. Similarly, if $\hat{n}_t < n_t$, the number of observed empty slots should be smaller than $\mu_t|_{\rho_t=1}$. In a different perspective, $\mu_t|_{\rho_t=1}$ can be regarded as ground truth used to determine the relationship of n_t and $\hat{n}_t$, as the empty slot probability is monotonous with n_t.

Motivated by the above observation, we design the active node population estimator that exploits the relationship of the number of empty slots observed by the Coordinator and the ground truth $\mu_t|_{\rho_t=1}$. **Let β_1 and β_2 be constants used to control the confidence interval and the adjusting frequency with $0 < \beta_2 \leq 1 \leq \beta_1$.** The estimate $\hat{W}_t$ is updated as follows:

$$\hat{W}_{t+1} = \begin{cases} \max\{1, \hat{W}_t - a_1\}, & \text{if } Y_t > \beta_1 \mu_t|_{\rho_t=1} \\ \hat{W}_t, & \text{if } Y_t \in [\beta_2, \beta_1]\mu_t|_{\rho_t=1} \\ \hat{W}_t + a_2, & \text{if } Y_t < \beta_2 \mu_t|_{\rho_t=1}, \end{cases} \quad (9)$$

where positive numbers a_1 and a_2 control the update step size. At frame t the Coordinator initially sets f_t and p_t to establish $\frac{f_t}{p_t} = \hat{n}_t$ using the estimate $\hat{W}_t$ obtained at the end of the previous frame. When frame t finishes, the Coordinator can measure the actual number of empty slots in this frame, and can adjust the estimate $\hat{W}_t$ following the rule in (9) through comparing the measured number of empty slots with $\mu_t|_{\rho_t=1}$. In particular, the estimator can be interpreted as follows:

1) If the estimate is accurate, i.e. $\hat{n}_t \approx n_t$ and $\rho_t \approx 1$, then it holds for the mean of Y_t that $\mu_t|_{\rho_t=1} \approx \frac{f_t}{e}$ following (3), where e is natural constant.
2) If the number of observed empty slots is more than $\beta_1 \mu_t|_{\rho_t=1}$, it indicates a higher value of $\hat{n}_t = \frac{f_t}{p_t}$, that is, $\hat{W}_t$ is overestimated. The Coordinator will thus decrease the estimate by a_1.
3) If the number of observed empty slots is smaller than $\beta_2 \mu_t|_{\rho_t=1}$, it indicates that $\hat{W}_t$ is underestimated. The Coordinator will thus increase the estimate by a_2.
4) If Y_t falls into the interval $[\beta_2 \mu_t|_{\rho_t=1}, \beta_1 \mu_t|_{\rho_t=1}]$ that is around $\mu_t|_{\rho_t=1}$, it suggests the estimate is felicitous, so the estimate stays unchanged.

Following the rule of the estimator, the estimate $\hat{W}_t$ would converge to the actual value of W_t with proper a_1, a_2, β_1 and β_2. The key challenge lies in setting them to guarantee the stability of SFP. In the following, we first present how to set a_1 and a_2, and leave the others for the next section.

C. Setting a_1 and a_2

The parameters a_1 and a_2 control the update step size and are crucial to guarantee the convergence of the estimator and the stability of SFP. Here, we design a_1 and a_2 by analyzing the drift of $\hat{W}_t$. To stabilize FSA-based systems, $\hat{W}_t$ needs to drift towards the number of actual nodes. As we focus on large-scale systems, W_t and $\hat{W}_t$ are large enough so that $\max\{1, \hat{W}_t - a_1\}$ in (9) can be approximated as $\hat{W}_t - a_1$.

Recall the update rule of the estimator in (9), the estimate evolves depending on W_t, $\hat{W}_t$, and f_t. When $W_t = n_t$ and its estimate $\hat{W}_t = \hat{n}_t$, let $\mu_t^* \triangleq \mu_t|_{\rho_t=1} = \frac{f_t}{e}$, the drift of estimate $\hat{W}_t$, defined by $\hat{D}$, can be formulated as

$$\hat{D}(n_t, \hat{n}_t, f_t) = E[\hat{W}_{t+1} - \hat{W}_t | W_t = n_t, \hat{W}_t = \hat{n}_t]$$
$$= \frac{-a_1}{\sqrt{2\pi}\sigma}\int_{\beta_1\mu^*}^{\infty} e^{\frac{-(y_t-\mu)^2}{2\sigma^2}} \mathrm{d}y_t + \frac{a_2}{\sqrt{2\pi}\sigma}\int_{-\infty}^{\beta_2\mu^*} e^{\frac{-(y_t-\mu)^2}{2\sigma^2}} \mathrm{d}y_t.$$

Setting $u = \frac{y_t - \mu}{\sigma}$ yields after algebraic operations

$$g(\rho_t, f_t) \triangleq \hat{D}(n_t, \hat{n}_t, f_t) = -a_1 + \frac{a_1}{\sqrt{2\pi}} \int_{-\infty}^{\phi_1(\rho_t, f_t)} e^{\frac{-u^2}{2}} \mathrm{d}u + \frac{a_2}{\sqrt{2\pi}} \int_{-\infty}^{\phi_2(\rho_t, f_t)} e^{\frac{-u^2}{2}} \mathrm{d}u, \quad (10)$$

where we make the following definitions

$$\phi_1(\rho_t, f_t) = \frac{\beta_1 \mu_t^* - \mu_t}{\sigma} = \frac{f_t^{\frac{1}{2}} \left(\beta_1 e^{-1} - e^{-\rho_t}\right)}{\left(e^{-\rho_t}(1 - e^{-\rho_t})\right)^{\frac{1}{2}}} \quad (11)$$

$$\phi_2(\rho_t, f_t) = \frac{\beta_2 \mu_t^* - \mu_t}{\sigma} = \frac{f_t^{\frac{1}{2}} \left(\beta_2 e^{-1} - e^{-\rho_t}\right)}{\left(e^{-\rho_t}(1 - e^{-\rho_t})\right)^{\frac{1}{2}}}. \quad (12)$$

It can be observed from (10) that the drift of the estimate $\hat{W}_t$ varies with ρ_t and f_t. Although the expression of ρ_t contains f_t, we can set such p_t that the value of $\frac{p_t}{f_t}$ does not vary with f_t, and the variation of f_t thus has no impact on the value of ρ_t. As a result, the impacts of ρ_t and f_t on $g(\rho_t, f_t)$ are independent mutually. That is to say, we can set f_t to a constant while varying p_t to decouple their impacts. The design of f_t will be addressed in the next section.

Since we seek to estimate W_t accurately, the value of ρ_t should be kept in the neighborhood of the optimal value $\rho_t^* = 1$. Meanwhile we also need to guarantee the convergence of the estimator, that is to say, $\hat{W}_t$ does not change on average, we thus should ensure that $g(\rho_t, f_t)|_{\rho_t = 1} = 0$, namely,

$$-a_1 + \frac{a_1}{\sqrt{2\pi}} \int_{-\infty}^{\phi_1(1, f_t)} e^{\frac{-u^2}{2}} \mathrm{d}u + \frac{a_2}{\sqrt{2\pi}} \int_{-\infty}^{\phi_2(1, f_t)} e^{\frac{-u^2}{2}} \mathrm{d}u = 0.$$

In order to make the equation above established, a_1 and a_2 need to satisfy the following condition:

$$\frac{a_1}{a_2} = \frac{\int_{-\infty}^{\phi_2(1, f_t)} e^{\frac{-u^2}{2}} \mathrm{d}u}{\int_{\phi_1(1, f_t)}^{\infty} e^{\frac{-u^2}{2}} \mathrm{d}u}. \quad (13)$$

Therefore, we configure a_1 and a_2 as follows:

$$a_1 = \gamma \int_{-\infty}^{\phi_2(1, f_t)} e^{\frac{-u^2}{2}} \mathrm{d}u \quad (14)$$

$$a_2 = \gamma \int_{\phi_1(1, f_t)}^{\infty} e^{\frac{-u^2}{2}} \mathrm{d}u, \quad (15)$$

where $\gamma > 0$ is the linear factor that controls the adjusting rate, we will evaluate its impact in Sec.V. With the selected a_1 and a_2, the estimator is able to guarantee that $g(1, f_t) = 0$. Hence, such a configuration provides a necessary condition to accurately track the number of active nodes.

Next, we further state the property of $g(\rho_t, f_t)$ in the following theorem indicating the estimate $\hat{W}_t$ will drift towards and will keep stable around its true value W_t when $\rho_t = \frac{W_t}{\hat{W}_t} \approx 1$.

Theorem 1: Given a_1 and a_2 formulated in (14) *and* (15)*, if $0 < \beta_2 \leq 1 \leq \beta_1 < e$, then it holds for the drift $g(\rho_t, f_t)$ of the estimator that*:

1) *$g(\rho_t, f_t)$ is a strictly increasing function of ρ_t.*
2) *$g(\rho_t, f_t) > 0$ when $\rho_t > 1$; $g(\rho_t, f_t) < 0$ when $\rho_t < 1$.*

Proof: Theorem 1 can be proven by calculating the derivative of $g(\rho_t, f_t)$ with respect to ρ_t. Since the impacts of ρ_t and f_t on $g(\rho_t, f_t)$ are independent mutually, we use $g(\rho_t)$, $\phi_1(\rho_t)$, and $\phi_2(\rho_t)$ in the rest of the paper for simplicity. Following from the property of the integral, we have

$$g'(\rho_t) = \frac{a_1}{\sqrt{2\pi}} e^{-\frac{\phi_1(\rho_t)^2}{2}} \phi_1'(\rho_t) + \frac{a_2}{\sqrt{2\pi}} e^{-\frac{\phi_2(\rho_t)^2}{2}} \phi_2'(\rho_t)$$

As shown in $g'(\rho_t)$, it is adequate to prove both $\phi_1'(\rho_t) > 0$ and $\phi_2'(\rho_t) > 0$ for the monotonic increase of $g(\rho_t)$.

Step 1: we prove $\phi_1'(\rho_t) > 0$.

Rewrite $\phi_1(\rho_t)$ as $\phi_1(\rho_t) = \frac{\sqrt{f_t}(\beta_1\ e^{\rho_t - 1} - 1)}{\sqrt{e^{\rho_t} - 1}}$, and we have

$$\phi_1'(\rho_t) = \sqrt{f_t} \left(\frac{\beta_1\ e^{\rho_t - 1}}{(e^{\rho_t} - 1)^{\frac{1}{2}}} - \frac{(\beta_1\ e^{\rho_t - 1} - 1)}{2(e^{\rho_t} - 1)^{\frac{3}{2}}} \right).$$

After some algebraic operations, we further get

$$\phi_1'(\rho_t) = \sqrt{f_t} e^{\rho_t} (e^{\rho_t} - 1)^{-\frac{3}{2}} \left(\frac{1}{2} + \frac{\beta_1 e^{\rho_t}}{2e} - \frac{\beta_1}{e} \right). \quad (16)$$

For $\sqrt{f_t} e^{\rho_t} (e^{\rho_t} - 1)^{-\frac{3}{2}} > 0$, it is adequate to show $\frac{1}{2} + \frac{\beta_1\ e^{\rho_t}}{2e} - \frac{\beta_1}{e} > 0$. As $e^{\rho_t} \geq 1$ when $\rho_t \geq 0$, it is true that

$$\frac{1}{2} + \frac{\beta_1\ e^{\rho_t}}{2e} - \frac{\beta_1}{e} \geq \frac{1}{2} - \frac{\beta_1}{2e}.$$

Hence, if $\beta_1 < e$, then $\phi_1'(\rho_t) > 0$ is established.

Step 2: we prove $\phi_2'(\rho) > 0$.

Similarly, we rewrite $\phi_2(\rho)$ as $\phi_2(\rho_t) = \frac{\sqrt{f_t}(\beta_2\ e^{\rho_t - 1} - 1)}{\sqrt{e^{\rho_t} - 1}}$. As the only difference between $\phi_2(\rho_t)$ and $\phi_1(\rho_t)$ is the value of β_1 and β_2, they have similar derivative. That is to say, if $\frac{1}{2} - \frac{\beta_2}{2e} > 0$, then $\phi_2'(\rho_t) > 0$ holds. Recall that we specify $\beta_2 \leq \beta_1$ in the estimator, $\beta_1 < e$ also establishes $\phi_2'(\rho_t) > 0$.

We now can conclude that $g(\rho_t)$ is a strictly increasing function of ρ_t. As a consequence, $g(\rho_t) > g(1) = 0$ when $\rho_t > 1$ and $g(\rho_t) < g(1) = 0$ when $\rho_t < 1$. □

The results stated in Theorem 1 reveal that $\rho_t = 1$ is the unique root of $g(\rho_t, f_t) = 0$. That is to say, if the estimator is accurate, $\hat{W}_t$ would drift toward to the true value W_t, eventually yielding $\rho_t = 1$. In order to understand better the behavior of $g(\rho_t, f_t)$, we also illustrate the impact of ρ_t on the drift in Fig. 2, which confirms our theoretical results.

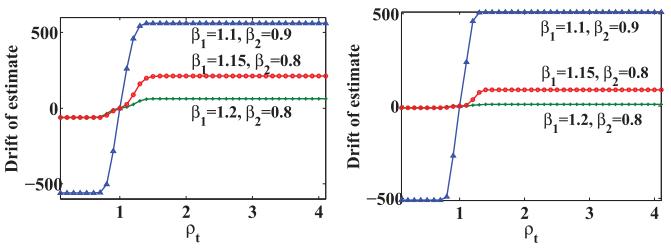

(a) $f_t = 200$ (b) $f_t = 400$

Fig. 2. Impact of ρ_t on the estimate drift: $\rho_t = 1$ is the unique root of $g(\rho_t, f_t) = 0$.

IV. Stability Analysis of SFP

In this section, we study the stability of SFP by employing drift analysis. Theoretically, we build a two-state Markov chain and analyze its geometrical ergodicity.

A. Markov Chain Formulation

As there are two key states evolving with time: the number of active nodes W_t and its estimate $\hat{W}_t$, we define a sequence $Z_t = (W_t, \hat{W}_t)$. Consider the overall new arrivals and the successful transmission in frame t, the dynamics of $\hat{W}_t$ and W_t can be formulated as (9) and (17)

$$W_{t+1} = \max\{0, W_t + A_t - S_t\}. \tag{17}$$

We can observe from (9) and (17) that the distribution of Z_{t+1} depends only on Z_t, meaning that the sequence Z_t is a Markov chain on a countable state space $\mathbb{S}_Z$. Having formulated the state dynamics, we next calculate the one-step state transition probability $\mathbf{P} = \{P_{n_t k}\ P_{\hat{n}_t k'}\}$. The transition probability $P_{\hat{n}_t k'}$ of $\hat{W}_t$ can be calculated from (9) as

$$P_{\hat{n}_t k'} = \begin{cases} \int_{\phi_1(\rho_t)}^{\infty} \frac{e^{\frac{-u^2}{2}}}{\sqrt{2\pi}} du, & \text{if } k' = \max(1, \hat{n}_t - a_1), \\ \int_{\phi_2(\rho_t)}^{\phi_1(\rho_t)} \frac{e^{\frac{-u^2}{2}}}{\sqrt{2\pi}} du, & \text{if } k' = \hat{n}_t, \\ \int_{-\infty}^{\phi_2(\rho_t)} \frac{e^{\frac{-u^2}{2}}}{\sqrt{2\pi}} du, & \text{if } k' = \hat{n}_t + a_2. \end{cases} \tag{18}$$

As shown in (17), W_t depends on both the number of arrivals and that of the successful transmissions. Let λ_i define the probability of having i arrivals and let $\xi_{n_t i}$ define the probability of having i successful transmissions in frame t. For different value of A_t and S_t, W_{t+1} may decrease, remain unchanged and increase. Hence, the transition probability of W_t can be formulated as

$$\begin{cases} P_{n_t k|n_t=0} = \begin{cases} \lambda_0, & k = 0 \\ \lambda_k, & k \geq 1, \end{cases} \\ P_{n_t k|n_t \geq 1} = \begin{cases} \sum_{i=0}^{k} \lambda_i \xi_{n_t, i+n_t-k}, & 0 \leq k < n_t, \\ \lambda_0 \xi_{n_t,0} + \sum_{i=1}^{n_t} \lambda_i \xi_{n_t i}, & k = n_t, \\ \sum_{i=0}^{n_t} \lambda_{i+k-n_t} \xi_{n_t i}, & k \geq n_t + 1, \end{cases} \end{cases} \tag{19}$$

where $\xi_{n_t,i} = \binom{f_t}{i} q_t^i(1)(1 - q_t(1))^{f_t - i}$. To show the stability of SFP, we need to prove the existence of steady distribution for each initial state of the formulated Markov chain $(Z_t)_{t\geq 0}$. As stated in Definition 1, this is equivalent to demonstrating the geometric ergodicity of $(Z_t)_{t\geq 0}$.

Before the formal stability analysis, we first introduce three auxiliary lemmas that will be used in the subsequent analysis.

Lemma 3 ([7]): A Markov chain on a countable state space (Z_t) is geometrically ergodic if it is irreducible and aperiodic, and has such a state z that the stopping time τ=$\min\{t > 0 : Z_t = z\}$ is exponential-type for any initial state Z_0.

Lemma 4 ([7]): Let $\{V_t\}$ be a sequence of random variables adapted to an increasing family $\{\mathcal{F}_t\}_{t\geq 0}$ of σ-algebras. If there exist such $d > 0$ and D that

$$E[e^{d|V_{t+1} - V_t|} | \mathcal{F}_t] \leq D, \quad \forall t \geq 0, \tag{20}$$

then it holds that $\{V_t, \mathcal{F}_t\}$ is exponential-type.

Lemma 5 ([7]): Under the same notations of Lemma 4, given an deterministic V_0 and that $\{V_t, \mathcal{F}_t\}$ is exponential-type, if it holds for some $\epsilon > 0$, $c > 0$ that [2]

$$E[V_{t+1} - V_t + \epsilon; V_t > c | \mathcal{F}_t] \leq 0, \quad \forall t \geq 0, \tag{21}$$

the stopping time $\tau = \min\{t \geq 0 : V_t \leq c\}$ is then exponential-type for each value of V_0.

These lemmas indicate that the ergodicity of Z_t can be established if we can find a V_t adapted to σ-field $\mathcal{F}_t$ generated by Z_t such that the lemmas above hold.

B. Stability Analysis

The main result described in Theorem 2 reveals the geometric ergodicity of $(Z_t)_{t\geq 0}$, which means the exponential-type stopping time for any initial state.

Theorem 2: Given a_1 and a_2 as in (14) *and* (15) *and $0 < \beta_2 \leq 1 \leq \beta_1 \leq e/2$, if $\lambda < e^{-1}$ and there exists a combination of $\beta_1, \beta_2, f_t, \gamma$ establishing* (37)*, then Markov chain $(Z_t)_{t\geq 0}$ is geometrically ergodic.*

Proof: The core idea underlaying the proof of the theorem is to employ the properties of the Markov chain $(Z_t)_{t\geq 0}$ to build a Lyapunov function with a negative drift. The skeleton of the proof can be summarized as follows:

- First, we prove the irreducibility and aperiodicity of Markov chain $Z_t = (W_t, \hat{W}_t)_{t\geq 0}$.
- Second, we study the properties of one-frame drift of $(Z_t)_{t\geq 0}$ which are used to prove the stability.
- Third, we develop drift analysis on constructed Lyapunov function to show that the J-frame drift is negative for some integer J, which is sufficient to ensure the geometric ergodicity of $(Z_t)_{t\geq 0}$.

Step 1: Irreducibility and aperiodicity of $(\hat{W}_t)_{t\geq 0}$. Given the value of W_t and $\hat{W}_t$, from (18) and (19), it is obvious that $(Z_t)_{t\geq 0}$ is irreducible and aperiodic according to their individual definitions if $0 < \lambda_i < 1$ for $\forall\ t \geq 0$. We would like to explain that most of traffic models can satisfy such a λ_i. Hence, the proof in this step follows from here.

Step 2: Properties of drifts. In order to evaluate the stability of SFP, we study the expected change of Z_t from frame t to frame $t + 1$. The convergence of the estimation error is crucial for the stability of a scheme. Denote by $\tilde{W}_t = \hat{W}_t - W_t$ the estimation error of the active node population estimator. Besides the drift of the estimator $\hat{D}(n_t, \hat{n}_t, f_t)$, we further define drifts of W_t and $\tilde{W}_t$ as:

$$D(n_t, \hat{n}_t, f_t) = E[W_{t+1} - W_t | Z_t = \{n_t, \hat{n}_t, f_t\}], \tag{22}$$

$$\begin{aligned} \tilde{D}(n_t, \hat{n}_t, f_t) &= E[\tilde{W}_{t+1} - \tilde{W}_t | Z_t = \{n_t, \hat{n}_t, f_t\}] \\ &= \hat{D}(n_t, \hat{n}_t, f_t) - D(n_t, \hat{n}_t, f_t). \end{aligned} \tag{23}$$

Recall the evolution of W_t shown in (17), we have

$$D(n_t, \hat{n}_t, f_t) = E[A_t - S_t] = f_t(\lambda - \rho_t e^{-\rho_t}). \tag{24}$$

[2]If Y is a random variable and A is an event, the notation $E[Y; A|\mathcal{F}]$ stands for $E[Y I_A|\mathcal{F}]$, where I_A is the indicator function of the event A.

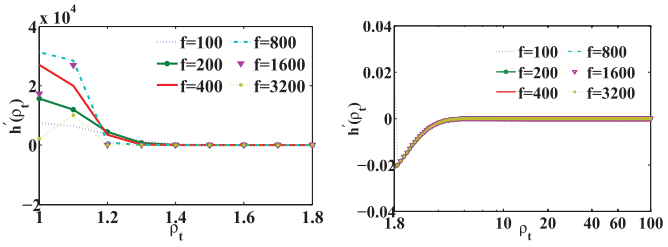

(a) $1 \le \rho_t \le 1.8$ (b) $1.8 \le \rho_t \le 100$

Fig. 3. Impact of ρ_t on the derivative of $h(\rho_t)$.

Hence, with (10) $\tilde{D}(n_t, \hat{n}_t, f_t)$ can be formulated as

$$\begin{aligned}\tilde{D}(n_t, \hat{n}_t, f_t) &= -a_1 + \frac{a_1}{\sqrt{2\pi}} \int_{-\infty}^{\phi_1(\rho_t)} e^{\frac{-u^2}{2}} \mathrm{d}u \\ &\quad + \frac{a_2}{\sqrt{2\pi}} \int_{-\infty}^{\phi_2(\rho_t)} e^{\frac{-u^2}{2}} \mathrm{d}u - f_t(\lambda - \rho_t e^{-\rho_t}). \end{aligned} \tag{25}$$

With the formula of $\tilde{D}(n_t, \hat{n}_t, f_t)$, we proceed to investigate its properties that are stated in the lemma below. **Let ρ_t^* be the root of** $h(\rho_t) \triangleq \tilde{D}(n_t, \hat{n}_t, f_t) = 0$, the proof is detailed in Appendix A. In order to understand behavior of $h(\rho_t)$, in addition to theoretical analysis, we also illustrate in Fig. 3 its derivative when $\rho_t \ge 1$ with $f_t = f = 100 : 3200$ and $(\beta_1 = 1.05, \beta_2 = 0.93, \gamma = 25)$, showing that $h(\rho_t)$ increases at first and then decreases to $\lim_{\rho_t \to \infty} h(\rho_t)$. This also verifies the theoretical results. Moreover, we can also observe that a longer frame will lead to a smaller $\overline{\rho}_t$ that satisfies $h'(\rho_t = \overline{\rho}_t) > 0$ and $h'(\rho_t > \overline{\rho}_t) < 0$.

Lemma 6: There exist $\beta_1, \beta_2, f_t, \gamma$ in (14) *and* (15) *establishing* (37) *such that $h(\rho_t)$ satisfies that*

- *$h(\rho_t)$ is increasing when $\rho_t \le 1$;*
- *$h(\rho_t) \ge h(1)$ when $\rho_t > 1$.*
- *for $\forall \lambda \in (0, e^{-1})$, there exists a unique $\rho_t \in (0, 1)$ such that $h(\rho_t) = 0$.*
- *if $\lambda \in (0, e^{-1})$ and $h(\rho_t^*) = 0$, then $\lambda < \rho_t^* e^{-\rho_t^*}$.*

Step 3: Stability analysis based on Lyapunov function. Recall the nature of $h(\rho_t)$ as the drift of estimate error which primarily depends on $\rho_t = \frac{n_t}{\hat{n}_t}$ for large values of $\hat{n}$ or n. Thus, given any $\zeta \in (0, 1)$ and an integer $M > 0$, with the assumption that $n_t \ge M$ holds for the rest of this paper, we partition state space into the following regions:

$$\begin{cases} \mathbb{G}_{\zeta,M} = \{(n_t, \hat{n}_t) : n_t \ge M \cup \hat{n}_t \ge M, \frac{n_t}{\hat{n}_t} \in [\rho_t^*\text{-}\zeta, 1 + \zeta]\}, \\ \mathbb{R}^+_{\zeta,M} = \{(n_t, \hat{n}_t) : n_t \ge M, \frac{n_t}{\hat{n}_t} > 1 + \zeta\}, \\ \mathbb{R}^-_{\zeta,M} = \{(n_t, \hat{n}_t) : \hat{n}_t \ge M, \frac{n_t}{\hat{n}_t} < \rho_t^* - \zeta\}, \\ \mathbb{Q}_M = \{(n_t, \hat{n}_t) : n_t < M, \hat{n}_t < M\}, \end{cases}$$

and let $\mathbb{R}_{\zeta,M} = \mathbb{R}^+_{\zeta,M} \cup \mathbb{R}^-_{\zeta,M}$.

Referring to the property of $h(\rho_t)$ stated in Lemma 6, we can derive the following results whose proof is presented in Appendix B. Lemma 7 can be interpreted as follows: Once exceeding a threshold, the deviation of the estimate $\hat{W}_t$ from W_t is expected to decrease, which guarantees the stability.

Lemma 7: There exist $\zeta \in (0, \frac{1}{5})$, $\delta > 0$ and an integer $M > 0$ such that

$$D(n_t, \hat{n}_t) \le -\delta, \quad \forall\, (n_t, \hat{n}_t) \in \mathbb{G}^+_{5\zeta,M}, \tag{26}$$

$$\tilde{D}(n_t, \hat{n}_t) \ge \delta, \quad \forall\, (n_t, \hat{n}_t) \in \mathbb{R}^+_{\zeta,M}, \tag{27}$$

$$\tilde{D}(n_t, \hat{n}_t) \le -\delta, \quad \forall\, (n_t, \hat{n}_t) \in \mathbb{R}^-_{\zeta,M}. \tag{28}$$

Now, we initiate the drift analysis. We fix ζ, δ and M such that (26), (27) and (28) hold. Motivated by Lemmas 4 and 5, we choose the following Lyapunov function,

$$\begin{aligned} V(n_t, \hat{n}_t) &= \max\Big\{n_t, \frac{1+3\zeta}{3\zeta}(n_t\text{-}\hat{n}_t), \frac{(\rho_t^*\text{-}3\zeta)(\hat{n}_t\text{-}n_t)}{1\text{-}\rho_t^* + 3\zeta}\Big\} \\ &= \begin{cases} n_t, & \text{if } (n_t, \hat{n}_t) \in \mathbb{G}_{3\zeta,M}, \\ \frac{1+3\zeta}{3\zeta}(n_t - \hat{n}_t), & \text{if } (n_t, \hat{n}_t) \in \mathbb{R}^+_{3\zeta,M}, \\ \frac{\rho_t^* - 3\zeta}{1 - \rho_t^* + 3\zeta}(\hat{n}_t - n_t), & \text{if } (n_t, \hat{n}_t) \in \mathbb{R}^-_{3\zeta,M}. \end{cases} \end{aligned} \tag{29}$$

for two reasons: First, it is exponential-type. As $|\hat{W}_{t+1} - \hat{W}_t| \le \max\{a_1, a_2\}$ and $|W_{t+1} - W_t| < \max\{A_t, f_t\}$, then we have $|V(n_{t+1}, \hat{n}_{t+1}) - V(n_t, \hat{n}_t)| \le \frac{1+3\zeta}{3\zeta} \cdot \max\{a_1, a_2, A_t, f_t\}$, yielding that $V(n_t, \hat{n}_t)$ is exponential-type since A_t is. Second, V can take best advantage of the drift properties proven in Lemma 7. For example, when $Z_t = (n_t, \hat{n}_t)$ belongs to $\mathbb{G}_{2\zeta,M}$, then $Z_{t+1} = (n_{t+1}, \hat{n}_{t+1})$ falls into $\mathbb{G}_{3\zeta,M}$, and the one-frame drift $E[V(n_{t+1}, \hat{n}_{t+1}) - V(n_t, \hat{n}_t) | Z_t = (n_t, \hat{n}_t)]$ is negative. Similar results can also hold for $\mathbb{R}_{4\zeta,M}$.

Yet Z_{t+1} may jump to a different region when Z_t is close to the boundary between adjacent regions. Fortunately, we can prove the negativity of J-frame drift of V, which is adequate to prove geometric ergodicity. To that end, the key is to prove

$$E[V(n_{t+J}, \hat{n}_{t+J}) - V(n_t, \hat{n}_t) | (n_t, \hat{n}_t) \notin \mathbb{Q}_{M+J^2}] \le -\epsilon, \tag{30}$$

for a large enough J and some $\epsilon > 0$. To that end, we define a random variable τ_J by

$$\tau_J = \min\{s \ge t : \sum_{k=t}^{t+s} A_k \ge J\}, \tag{31}$$

where A_k is the number of new arrivals at frame k. Similar to [12], the proof consists of two parts: considering unlikely event $\tau_J \le J$ and likely event $\tau_J > J$. We start with the unlikely event. Following Chernoff bound, we can obtain two results:

$$\lim_{J \to \infty} JP(\tau_J \le J) = 0, \tag{32}$$

$$\lim_{J \to \infty} E\Big[m_1 J + m_2 \sum_{k=t}^{t+J} A_k; \tau_J \le J\Big] = 0, \tag{33}$$

where m_1 and m_2 are arbitrary given constants. Thus

$$\begin{aligned} &|V(n_{t+1}, \hat{n}_{t+1}) - V(n_t, \hat{n}_t)| \\ &\le \frac{1+3\zeta}{3\zeta}\{a_1 + a_2 + A_t + f_t\} \\ &\le \frac{1+3\zeta}{3\zeta}(a_1 + a_2 + f_t)J + \frac{1+3\zeta}{3\zeta} \sum_{k=t}^{t+J} A_k \to 0, \end{aligned} \tag{34}$$

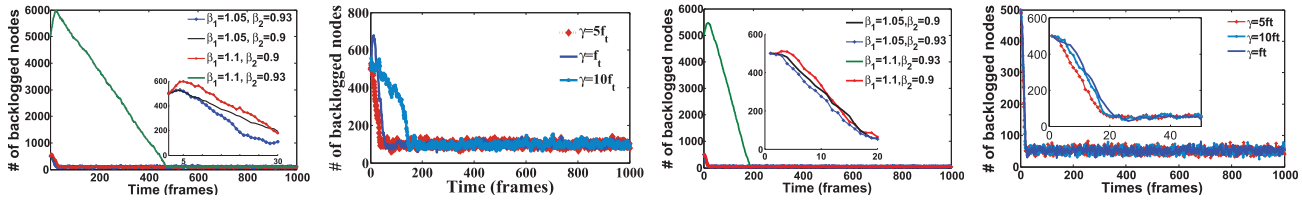

(a) Impact of β_1 and β_2: $\lambda = 0.3$ (b) Impact of γ: $\lambda = 0.3$ (c) Impact of β_1 and β_2: $\lambda = 0.2$ (d) Impact of γ: $\lambda = 0.2$

Fig. 4. The impact of the estimator parameters on SFP performance.

following from (33) when J is large enough.

We next consider likely event. Specifically, we conduct drift analysis in the five cases when the state space are divided into five region: $\mathbb{G}_{2\zeta,M+J^2}$, $\mathbb{R}^+_{4\zeta,M+J^2}$, $\mathbb{R}^-_{4\zeta,M+J^2}$, $\mathbb{G}_{5\zeta,M+J^2} \cap \mathbb{R}^+_{\zeta,M+J^2}$, $\mathbb{G}_{5\zeta,M+J^2} \cap \mathbb{R}^-_{\zeta,M+J^2}$. Following the approach in [12], we can prove that (30) holds in any cases for large enough J. Since the one-frame drift is negative if Z_{t+1} falls into a subspace of that contains Z_t, according to the properties stated in Lemma 7, we mainly consider the more complicated cases, namely the last two cases, that is to say, the subcases: $\rho_t \in (1+2\zeta, 1+4\zeta]$ and $\rho_t \in (\beta-4\zeta, \beta-2\zeta]$. As the properties in these two region are identical, we only show the proof of the first subcase.

Consider $\rho_t \in (1+2\zeta, 1+4\zeta]$, we have $V(n_t, \hat{n}_t) = \max\{n_t, \frac{1+3\zeta}{3\zeta}(n_t - \hat{n}_t)\}$. Since $V(n_{t+J}, \hat{n}_{t+J})$ falls into $\mathbb{G}_{5\zeta,M+J^2} \cap \mathbb{R}^+_{\zeta,M+J^2}$ after J frames, it is true that $V(n_{t+J}, \hat{n}_{t+J}) = \max\{n_{t+J}, \frac{1+3\zeta}{3\zeta}(n_{t+J} - \hat{n}_{t+J})\}$.

In addition, $\tilde{W}_t = W_t - \hat{W}_t$, we thus have

$$\begin{aligned} &E[V(n_{t+J}, \hat{n}_{t+J}) - V(n_t, \hat{n}_t); \tau > J | (n_t, \hat{n}_t)] \\ &\le E[-\frac{J\delta}{2}; \tau > J] + E[\max\{0, n_{t+J} - n_t + \frac{J\delta}{2}; \tau > J\}] \\ &\quad + E[\max\{0, -\frac{1+3\gamma}{3\gamma}(\tilde{n}_{t+J} - \tilde{n}_t) + \frac{J\delta}{2}\}; \tau > J]. \end{aligned}$$

The inequality (30) holds in this subcase if we can show the right hand side is negative. To that end, we start with the study of the second item. Denote by $R_k = W_{t+k} - W_t + k\delta/2$, we have $|R_{k+1} - R_k| = |W_{t+k+1} - W_{t+k} + \delta/2| \le f_t + A_{t+k} + \delta/2$. Since A_{t+k} is exponential-type, $\{R_k, \mathcal{F}_{t+k}\}$ is also exponential-type where $\mathcal{F}_{t+k}$ is σ-field generated by $\{W_s, \hat{W}_s, A_{s-1} : s \le k+t\}$. Hence, $E[\max\{0, n_{t+J} - n_t + \frac{J\delta}{2}; \tau > J\}] \le B$ according to Proposition 2.2 in [12], where B is a constant independent of J. Similarly, the third item is also smaller than B. At last, the first item is equal to $-P(\tau_J > J)J\delta/2 \to -J\delta/2$ for a large enough J following (32). Finally, setting $\epsilon = -J\delta/2 + 2B < 0$ yields desired negative J-frame drift.

To conclude the proof, we set such a constant $\Theta = (M + J^2)\max\{1, \frac{1+3\zeta}{3\zeta}, \frac{\rho_t^* - 3\zeta}{1-\rho_t^*+\zeta}\}$ that the condition in (30) holds if $V(n_t, \hat{n}_t) > \Theta$. Therefore, the stopping time $\tau = \min\{t \ge 0 : V_t \le \Theta\}$ is exponential-type for any initial state following Lemma 5, and thus the Markov chain $(Z_t)_{t\ge 0}$ is geometrically ergodic, concluding the proof of Theorem 2. □

C. Parameter Configuration Rule

We conclude this section by explaining how to configure the parameters in SFP, containing the parameters of FSA and the active node population estimator. **This rule and the estimator and FSA mechanism together constitute SFP**.

1) Selection of β_1 and β_2: The more they concentrate around 1, the more accurate the estimate is at the cost of more frequent update and greater fluctuation. Hence, we pick moderate values for them that satisfy Theorem 2, for instance, $\beta_1 = 1.05$, $\beta_2 = 0.93$ in the simulation.
2) Selection of f_t and γ: In this paper, f_t is set to a constant over time which maximizes $\overline{p}_t$ in (36) while establishing the nonnegativity of (37) and ensuring $a_2 > f_t$ together with γ. Given f_t and the value of the estimate $\hat{n}_t$, we have the participation probability p_t set to $\frac{f_t}{\hat{n}_t}$.

As a result, we can obtain all parameters in SFP which guarantee the main results of this paper.

V. Simulation Results

In this section, we verify the performance of SFP. In order to confirm the tracking ability of SFP, the number of new arrivals per slot follows Poisson distribution with the expectation of 0.3 by default. The simulation settings follow the rule stated in Sec.IV-C, meeting the requirements of Theorem 1 and Theorem 2. The experiment lasts for $1,000$ frames.

A. Parameter Selection

We study the impact of β_1, β_2 and γ on SFP stability in terms of the number of backlogged nodes with the expected arrival rate per slot λ varied. The initial number of the nodes is 500, and the initial estimate and the constant frame size are set to 1 and 200, respectively. The participation probability is $p_t = \min\{1, f_t/\hat{n}_t\}$.

First, we fix $\gamma = 5f_t$. As shown in Fig. 4(a) and 4(c), only when both β_1 and β_2 are much closer to 1, SFP performs best. Otherwise, the convergence time sharply increases. The reason lies in that the former outputs more accurate estimate and thus more appropriate p_t for the throughput maximization. In addition, the impact of β_1 is more than β_2 when the estimate in the beginning is far smaller than the true value. This can be interpreted as follows: In the beginning, the estimate is much smaller than the true value, so we need to increase $\hat{W}_t$ with a step size of a_2. Recall that a_2 depends on β_1 in (15), a smaller $\beta_1 - 1$ yields a bigger a_2 and thus the speed that the estimate approaches the true is faster.

Given $\beta_1 = 1.05$ and $\beta_2 = 0.93$, we evaluate the impact of γ with its value set to $f_t, 5f_t, 10f_t$, respectively. We can

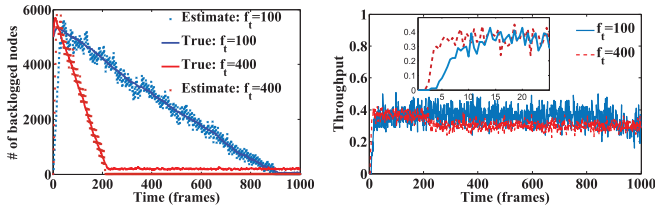

(a) True number of active nodes vs. estimate (b) Throughput under different f_t

Fig. 5. Performance evaluation with $5,000$ initial nodes under different f_t.

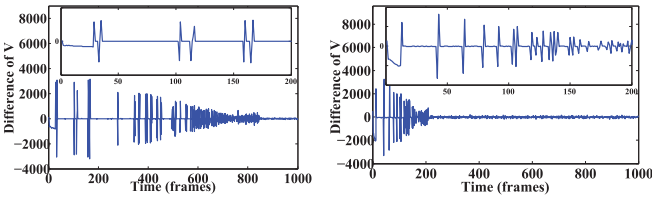

(a) $f_t = 100$ (b) $f_t = 400$

Fig. 6. Evolution of Lyapunov function $V(n_t, \hat{n}_t)$ with 5,000 initial nodes.

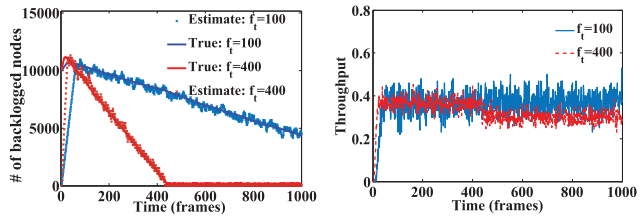

(a) True number of active nodes vs. estimate (b) Throughput under different f_t

Fig. 7. Performance evaluation with $10,000$ initial nodes under different f_t.

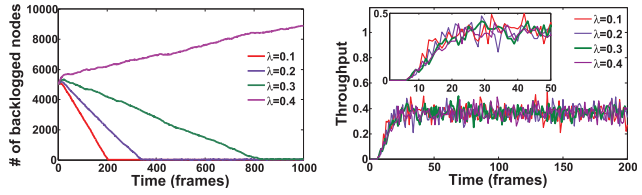

(a) True number of backlogged nodes vs. λ (b) Throughput under different λ

Fig. 8. Performance evaluation with $5,000$ initial nodes under different λ.

observe from Fig. 4(b) and 4(d) that SFP with $\gamma = 5f_t$ performs best. This can be interpreted as follows: The estimator with a small γ, e.g. $\gamma = f_t$, cannot adjust the estimate to its true value promptly while a big one, e.g. $\gamma = 10f_t$, results in an overlarge adjustment range and thus inaccurate estimate. In addition, Fig. 4 implies that the fewer new arrivals make the system more stable.

B. Performance Evaluation

Motivated by the observations above, we set $\beta_1 = 1.05$, $\beta_2 = 0.93$ and $\gamma = 5f_t$, and vary $f_t = 100, 400$ to further evaluate SFP through two groups of simulations in terms of estimation accuracy and throughput. When $f_t = 100$, we obtain $a_1 = 149$ and $a_2 = 176$; $a_1 = 286$ and $a_2 = 446$ when $f_t = 400$. In the first group of simulations, the initial number of the nodes is set to $5,000$. We record the estimation process and throughput in the duration, as depicted in Fig. 5(a) and Fig. 5(b). As shown in the figures, SFP does well in tracking the dynamics of node population and can achieve the throughput close to the optimal e^{-1}. In addition, we observe that the smaller frame size $f_t = 100$ leads to more accurate estimation and thus higher stationary throughput. This can be interpreted as follows: when $\rho_t > 1$, a smaller frame size results in a smaller update step sizes a_1 and a_2, thus it takes more frames for SFP to reach true number of nodes, but SFP experiences lighter fluctuations in steady state, for instance, after the 200th frame.

In the experiment, we also record the differences of the Lyapunov functions for two consecutive frames, i.e., $V(n_{t+1}, \hat{n}_{t+1}) - V(n_t, \hat{n}_t)$, and depict them in Fig. 6. It can be observed from the subfigures that difference will drop sharply once deviating far from zero towards the positive direction. This matches the analytical result on the negative J-frame drift of $V(n_t, \hat{n}_t)$ under SFP, which confirms the stability of SFP from another angle.

In order to examine the performance of SFP in larger system, we make the system scale up to $10,000$, and depict the results in Fig. 7(a) and Fig. 7(b). From the figures, we can observe that the conclusion drawn from Fig. 5 remains true here. Comparing Fig. 7 with Fig. 5, we can find that SFP with longer frame performs better in larger systems. In contrast, the number of the remaining backlogged nodes for $f_t = 100$ here is significantly bigger than that in Fig. 5.

We finally evaluate the performance of SFP with different arrival rates. As shown in Fig. 8(a) where λ changes from 0.1 to 0.4, the system is instable at $\lambda = 0.4$ when the condition $\lambda < e^{-1}$ of Theorem 2 is not satisfied. In contrast, the system is more stable under a smaller λ for $\lambda < e^{-1}$. Different from the impact of λ on the stability, it almost has no impact on the throughput, which can be observed from Fig. 8(b), because the throughput only depends on the protocol parameters.

VI. Related Work

In this section, we briefly review the related work. Globally speaking, the main research thrust in analyzing FSA is characterizing the performance of FSA-based systems in terms of delay, throughput and stability. However, none of the prior works provides a comprehensive treatment on the FSA stabilization in dynamic systems with new traffic arrivals and unknown node population.

Schoute [11] studied FSA with frame size configured dynamically and derived the expected time taken to send all backlogs. Wieselthier *et al.* [15] conducted performance analysis of FSA with multi-packet reception ability for small systems through a combinatorial technique. The optimal frame size setting for FSA was investigated in [1], [20], [21] with the assumption that the system is static and the number of nodes is known. *The works above neither address the stability of FSA nor work for communication systems with the new arrivals despite of their fundamental and practical importance.*

Gallego *et al.* analyzed throughput and time efficiency of reservation dynamic FSA for M2M communication systems with/without energy harvesting [13], [14]. Recently, George and Venkatesh [5], [6] investigated performance of M2M data collection systems using FSA as MAC protocol, and derived closed-form expressions for system throughput, packet delay, and energy efficiency. *However, these works assumed either no new arrivals or known number of nodes. Moreover, they did not address stability of FSA.* The sufficient conditions for the FSA stability were proven in our prior work [16]. *Yet this paper did not design an estimator that can stabilize FSA theoretically and thus left the impact of the estimator on stability of an FSA-based protocol unaddressed, which is the focus of our paper. We would like to emphasize that unified design and analysis in our work is more challenging.*

In summary, the stability and stabilization of FSA-based protocols are largely unaddressed, particularly for dynamic systems with new arrivals and unknown node population. In this regard, our work consists of a first step toward establishing a systematical framework that fills this void.

VII. Conclusion

In this paper, we have studied the problem of the design and stabilization of an FSA-based protocol with the presence of new arrivals and unknown node population. This problem has been addressed in two parts. First, we have proposed a stable protocol SFP that contains FSA mechanism and a node population estimator. Second, we have proven the stability of SFP by modeling dynamics of the node population and its estimate as a Markov chain and demonstrating its geometric ergodicity. The closed-form conditions on parameters of SFP have been derived for the stabilization when the average arrival rate should be smaller than e^{-1}. We have conducted experiments whose results match with the theoretical analysis. This paper presents the first work on stable FSA-based protocol for dynamic IoT systems like M2M and RFID with guaranteed stability theoretically.

Appendix A
Proof of Lemma 6

Proof: To prove this lemma, we calculate the derivative of $h(\rho_t) = \tilde{D}$.

(1) We start with the proof of the first property. Because it holds for $\forall \rho_t > 0$ that ${\phi_1}'(\rho_t) > 0$ and ${\phi_2}'(\rho_t) > 0$, it is easy to check that the first item in the right hand of the following $h'(\rho_t)$ is non-negative if $\rho_t \leq 1$. As a result, $h(\rho_t)$ is monotonically increasing for $\rho_t \leq 1$.

$$h'(\rho_t) = f_t(1-\rho_t)e^{-\rho_t} + \frac{a_1}{\sqrt{2\pi}} e^{-\frac{\phi_1(\rho_t)^2}{2}} {\phi_1}'(\rho_t) + \frac{a_2}{\sqrt{2\pi}} e^{-\frac{\phi_2(\rho_t)^2}{2}} {\phi_2}'(\rho_t) \quad (35)$$

(2) We prove the second property. Yet it is too complicated to study whether $h'(\rho_t) > 0$ for all $\rho_t > 1$. We conduct the proof in two steps. First, we show $h'(\rho_t) > 0$ when ρ_t falls into $[1, \overline{\rho}_t]$ where $\overline{\rho}_t \leq 2$. To that end, algebraically we get:

$$\begin{cases} \dfrac{-\phi_1(\rho_t)^2}{2} = -\dfrac{f_t(\frac{\beta_1}{e}e^{\rho_t}-1)^2}{2(e^{\rho_t}-1)} \geq -\dfrac{f_t(\frac{\beta_1}{e}e^{\overline{\rho}_t}-1)^2}{2(e^{\overline{\rho}_t}-1)} \\ \dfrac{-\phi_2(\rho_t)^2}{2} \geq -\max\{\dfrac{f_t(\frac{\beta_2}{e}e^{\overline{\rho}_t}-1)^2}{2(e^{\overline{\rho}_t}-1)}, \dfrac{f_t(\beta_2-1)^2}{2(e-1)}\} \end{cases}$$

for $\rho_t \geq 1$. we also have:

$$\begin{cases} {\phi_1}'(\rho_t) = \sqrt{f_t}e^{\rho_t}(e^{\rho_t}-1)^{-\frac{3}{2}}(\dfrac{1}{2} + \dfrac{\beta_1 e^{\rho_t}}{2e} - \dfrac{\beta_1}{e}) > \dfrac{\sqrt{f_t}\beta_1}{2\sqrt{e}} \\ {\phi_2}'(\rho_t) = \sqrt{f_t}e^{\rho_t}(e^{\rho_t}-1)^{-\frac{3}{2}}(\dfrac{1}{2} + \dfrac{\beta_2 e^{\rho_t}}{2e} - \dfrac{\beta_2}{e}) > \dfrac{\sqrt{f_t}\beta_2}{2\sqrt{e}} \end{cases}$$

if $\beta_1 \leq \frac{e}{2}$. Accordingly, it is sufficient to prove that

$$f_t(\rho_t-1)e^{-\rho_t} \leq \frac{a_2\beta_2\sqrt{f_t}}{2\sqrt{2e\pi}} e^{-\max\{\frac{f_t(\frac{\beta_2}{e}e^{\overline{\rho}_t}-1)^2}{2(e^{\overline{\rho}_t}-1)}, \frac{f_t(\beta_2-1)^2}{2(e-1)}\}} + \frac{a_1\beta_1\sqrt{f_t}}{2\sqrt{2e\pi}} e^{-\frac{f_t(\frac{\beta_1}{e}e^{\overline{\rho}_t}-1)^2}{2(e^{\overline{\rho}_t}-1)}}, \quad (36)$$

for $1 \leq \rho_t \leq \overline{\rho}_t$, where the right hand side increases when $\bar{\rho}_t \leq 2$. Therefore, given a_1, a_2, $\beta 1$, $\beta 2$ and f_t, we can obtain such $\overline{\rho}_t$ that $h(\rho_t)$ is monotonically increasing for $1 \leq \rho_t \leq \overline{\rho}_t$.

To get more accurate $\overline{\rho}_t$, we can search for the first $\rho_t = \overline{\rho}_t$ that results in $h'(\overline{\rho}_t) \geq 0$ and $h'(\rho_t > \overline{\rho}_t) < 0$ because $h'(\rho_t) > 0$ for $\rho_t \leq 1$ and $h(\rho_t)$ is continuous. Following the properties of Normal distribution and the fact that both $g(\rho_t)$ and $f_t(\lambda - \rho_t e^{-\rho_t})$ are monotonically increasing when $\rho_t \geq 1$, it is adequate to search in the region $[1, 10]$ when $g(\rho_t)$ will converge to a_2. $h(\rho_t)$ is thus increasing in $[1, \overline{\rho}_t]$.

With such $\overline{\rho}_t$, we compare $h(\rho_t)$ with $h(1)$ for $\rho_t > \overline{\rho}_t$:

$$\begin{aligned} &h(\rho_t) - h(1) \\ &= g(\rho_t) - f_t(e^{-1} - \rho_t e^{-\rho_t}) \\ &> -\frac{a_1}{\sqrt{2\pi}} \int_{\phi_1(\overline{\rho}_t)}^{\infty} e^{\frac{-u^2}{2}} \mathrm{d}u \\ &\quad + \frac{a_2}{\sqrt{2\pi}} \int_{-\infty}^{\phi_2(\overline{\rho}_t)} e^{\frac{-u^2}{2}} \mathrm{d}u - \frac{f_t}{e}. \end{aligned} \quad (37)$$

Hence, setting a_1, a_2, $\beta 1$, $\beta 2$ and f_t to guarantee nonnegativity of the above inequality yields that $h(\rho_t) \geq h(1)$.

(3) We then prove the third property. Due to the fact that $h(\rho_t) \to -f_t\lambda < 0$ when $\rho_t \to 0$, and $h(\rho_t > 1) \geq h(1) = f_t(e^{-1} - \lambda) > 0$, solutions to $h(\rho_t) = 0$ fall into $(0, 1)$ where $h(\rho_t)$ increases monotonically, there thus exists a unique solution.

(4) Finally, given $\lambda \in (0, e^{-1})$, we have $g(\rho_t^*) < 0$ because of the solution $\rho_t^* < 1$. As $h(\rho_t^*) = 0$, it holds that $-f_t(\lambda - \rho_t^* e^{-\rho_t^*}) > 0$, meaning $\lambda < \rho_t^* e^{-\rho_t^*}$. □

Appendix B
Proof of Lemma 7

Proof: For $(n_t, \hat{n}_t) \in \mathbb{G}^+_{5\zeta, M}$ where $\rho_t^* - 5\zeta \leq \rho_t = \frac{n}{\hat{n}} \leq 1 + 5\zeta$, recall that $\lambda - \rho_t e^{-\rho_t} < 0$ when $\rho_t = 1$ and $\rho_t = \rho_t^*$, and it is continuous and increasing monotonically in the range $[\rho_t^*, 1]$, there thus exist some γ and δ such that $D(n_t, \hat{n}_t) \leq -\delta$ for all $\rho_t \in [\rho_t^* - 5\zeta, 1 + 5\zeta]$.

If $(n_t, \hat{n}_t) \in \mathbb{R}^+_{\zeta,M}$ where $\rho_t = \frac{n_t}{\hat{n}_t} > 1 + \zeta > 1$, we have $h(\rho_t) \geq h(1) > 0$ which indicates that $\tilde{D}(n_t, \hat{n}_t) = h(\rho_t) \geq \delta$ for all $\rho_t > 1 + \gamma$. If $(n_t, \hat{n}_t) \in \mathbb{R}^-_{\zeta,M}$ where $\rho_t = \frac{n_t}{\hat{n}_t} < \rho_t^* - \zeta < \rho_t^*$, we have $h(\rho_t) \leq h(\rho_t^* - \zeta) < 0$, which indicates that $h(\rho_t \leq \rho_t^* - \zeta) \leq -\delta$. □

REFERENCES

[1] L. Barletta, F. Borgonovo, and M. Cesana, "A formal proof of the optimal frame setting for dynamic-frame aloha with known population size," *IEEE Trans. Inf. Theory*, vol. 60, no. 11, pp. 7221–7230, Nov. 2014.

[2] E. Elbasani, P. Siriporn, and J. S. Choi, "A survey on RFID in industry 4.0," in *Internet Things for Ind. 4.0*. Cham, Switzerland: Springer, 2020, pp. 1–16.

[3] *Radio-Frequency Identity Protocols Class-1 Generation-2 UHF RFID Protocol for Communications at 860 mhz-960 mhz Version 1.0.9*, EPCglobal, Brussels, Belgium, 2005, vol. 17.

[4] O. Galinina, A. Turlikov, S. Andreev, and Y. Koucheryavy, "Stabilizing multi-channel slotted ALOHA for machine-type communications," in *Proc. IEEE Int. Symp. Inf. Theory*, Jul. 2013, pp. 2119–2123.

[5] A. George and T. G. Venkatesh, "Performance analysis of M2M data collection networks using dynamic frame-slotted ALOHA," *IEEE Trans. Green Commun. Netw.*, vol. 2, no. 2, pp. 493–505, Jun. 2018.

[6] A. George and T. G. Venkatesh, "Efficiency analysis of M2M data collection networks using multipacket reception in frame-slotted ALOHA," in *Proc. IEEE Wireless Commun. Netw. Conf.*, Apr. 2016, pp. 1–6.

[7] B. Hajek, "Hitting-time and occupation-time bounds implied by drift analysis with applications," *Adv. Appl. Probab.*, vol. 14, no. 03, pp. 502–525, Sep. 1982.

[8] M. Mitzenmacher and E. Upfal, *Probability and Computing: Randomized Algorithms and Probabilistic Analysis*. Cambridge, U.K.: Cambridge Univ. Press, 2005.

[9] V. Naware, G. Mergen, and L. Tong, "Stability and delay of finite-user slotted ALOHA with multipacket reception," *IEEE Trans. Inf. Theory*, vol. 51, no. 7, pp. 2636–2656, Jul. 2005.

[10] M. R. Palattella *et al.*, "Internet of things in the 5G era: Enablers, architecture, and business models," *IEEE J. Sel. Areas Commun.*, vol. 34, no. 3, pp. 510–527, Mar. 2016.

[11] F. Schoute, "Dynamic frame length ALOHA," *IEEE Trans. Commun.*, vol. 31, no. 4, pp. 565–568, Apr. 1983.

[12] J. Tsitsiklis, "Analysis of a multiaccess control scheme," *IEEE Trans. Autom. Control*, vol. 32, no. 11, pp. 1017–1020, Nov. 1987.

[13] F. Vazquez-Gallego, J. Alonso-Zarate, and L. Alonso, "Reservation dynamic frame slotted-ALOHA for wireless M2M networks with energy harvesting," in *Proc. IEEE Int. Conf. Commun. (ICC)*, Jun. 2015, pp. 5985–5991.

[14] F. Vazquez-Gallego, J. Alonso-Zarate, A. M. Mandalari, O. Briante, A. Molinaro, and G. Ruggeri, "Performance evaluation of reservation frame slotted-ALOHA for data collection M2M networks," in *Proc. 20th Eur. Wireless Conf.*, Barcelona, Spain, May 2014, pp. 1–6.

[15] J. E. Wieselthier, A. Ephremides, and L. A. Michaels, "An exact analysis and performance evaluation of framed ALOHA with capture," *IEEE Trans. Commun.*, vol. 37, no. 2, pp. 125–137, 1989.

[16] J. Yu and L. Chen, "Stability analysis of frame slotted ALOHA protocol," *IEEE Trans. Mobile Comput.*, vol. 16, no. 5, pp. 1462–1474, May 2017.

[17] J. Yu, W. Gong, J. Liu, L. Chen, K. Wang, and R. Zhang, "Missing tag identification in COTS RFID systems: Bridging the gap between theory and practice," *IEEE Trans. Mobile Comput.*, vol. 19, no. 1, pp. 130–141, Jan. 2020.

[18] J. Yu, J. Liu, R. Zhang, L. Chen, W. Gong, and S. Zhang, "Multi-seed group labeling in RFID systems," *IEEE Trans. Mobile Comput.*, early access, Aug. 14, 2019, doi: 10.1109/TMC.2019.2934445.

[19] P. Zhang, H. Liu, and J. Yu, "On efficient key tag writing in RFID-enabled IoT," *China Sci. Inf. Sci.*, to be published. [Online]. Available: https://engine.scichina.com/publisher/scp/journal/SCIS/doi/10.1007/s11432-019-2891-3?slug=abstract, doi: 10.1007/s11432-019-2891-3.

[20] L. Zhu and T. P. Yum, "Optimal frame ALOHA-based anti-collision algorithm for rfid systems," *IEEE Trans. Commun.*, vol. 58, no. 12, pp. 3583–3592, Nov. 2010.

[21] L. Zhu and T.-S. Yum, "A critical survey and analysis of RFID anti-collision mechanisms," *IEEE Commun. Mag.*, vol. 49, no. 5, pp. 214–221, May 2011.

Jihong Yu (Member, IEEE) received the B.E. and M.E. degrees from the Chongqing University of Posts and Telecommunications, Chongqing, China, in 2010 and 2013, respectively, and the Ph.D. degree in computer science from the University of Paris-Sud, Orsay, France, in 2016. He was a Post-Doctoral Researcher with the School of Computing Science, Simon Fraser University, Canada. He is currently a Professor with the School of Information and Electronics, Beijing Institute of Technology. His research interests include RFID, backscatter networking, and Internet of Things.

Pengfei Zhang received the B.E. degree from Central South University, Changsha, China, in 2010, and the M.E. degree from Tsinghua University, Beijing, China, in 2014. He is currently pursuing the Ph.D. degree with the Beijing Institute of Technology, Beijing. His research interests include RFID technology and Internet of Things.

Lin Chen (Member, IEEE) received the B.E. degree in radio engineering from Southeast University, China, in 2002, the Engineer Diploma degree from Telecom ParisTech, Paris, in 2005, and the M.S. degree in networking from the University of Paris. He is currently working as a Professor with the School of Computer Science and Technology, Sun Yat-sen University, and used to be an Associate Professor with the Department of Computer Science, University of Paris-Sud. His main research interests include modeling and control for wireless networks, distributed algorithm design, and game theory. He serves as the Chair of IEEE Special Interest Group on Green and Sustainable Networking and Computing with Cognition and Cooperation, and the IEEE Technical Committee on Green Communications and Computing.

Jiangchuan Liu (Fellow, IEEE) received the B.Eng. degree *(cum laude)* from Tsinghua University, Beijing, China, in 1999, and the Ph.D. degree from The Hong Kong University of Science and Technology in 2003.

He is currently a Full Professor (with University Professorship) with the School of Computing Science, Simon Fraser University, Burnaby, BC, Canada. He is an NSERC E. W. R. Steacie Memorial Fellow. He is a Steering Committee Member of the IEEE TRANSACTIONS ON MOBILE COMPUTING, and an Associate Editor of the IEEE/ACM TRANSACTIONS ON NETWORKING, the IEEE TRANSACTIONS ON BIG DATA, and the IEEE TRANSACTIONS ON MULTIMEDIA. He was a co-recipient of the Test of Time Paper Award of the ACM Multimedia Best Paper Award in 2012, the ACM TOMCCAP Nicolas D. Georganas Best Paper Award in 2013, and the IEEE INFOCOM in 2015.

Rongrong Zhang received the B.E. and M.E. degrees in communication and information systems from the Chongqing University of Posts and Telecommunications, Chongqing, China, in 2010 and 2013, respectively, and the Ph.D. degree in computer science from the University of Paris Descartes, France, in 2017. She was a Research Fellow with the School of Electrical Engineering and Computer Science, University of Ottawa, Ottawa, ON, Canada. She is currently an Associate Professor with Capital Normal University, Beijing, China. Her research interests focus on wireless body area networks and Internet of Things.

Kehao Wang received the B.S. degree in electrical engineering and the M.S. degree in communication and information system from the Wuhan University of Technology, Wuhan, China, in 2003 and 2006, respectively, and the Ph.D. degree with the Department of Computer Science, University of Paris-Sud XI, Orsay, France, in 2012. He is currently working as an Associate Professor with the Department of Information Engineering, Wuhan University of Technology. His research interests are cognitive radio networks and wireless network resource management.

Jianping An (Member, IEEE) received the Ph.D. degree from the Beijing Institute of Technology, China, in 1996. He joined the School of Information and Electronics, Beijing Institute of Technology in 1995, where he is currently a Full Professor and the Dean. His research interests are in the field of digital signal processing, wireless networks, and high-dynamic broadband wireless transmission technology.